Supplementary information for

Relevance of electron transfer pathway in photodynamic activity of Ru(II) polypyridyl complexes containing 4,7-diphenyl-1,10-phenanthroline ligands under normoxic and hypoxic conditions

Olga Mazuryk[a*], Ewelina Janczy-Cempa[a], Justyna Lagoszz[a], Dorota Rutkowska-Zbik[b], Agata Machnicka[a], Aneta Krasowska[a], Piotr Pietrzyk[a], Grażyna Stochel[a], Małgorzata Brindell[a]

[a]*Department of Inorganic Chemistry, Faculty of Chemistry, Jagiellonian University in Kraków, Gronostajowa 2, 30-387 Krakow, Poland, e-mail: mazuryk@chemia.uj.edu.pl*
[b]*Jerzy Haber Institute of Catalysis and Surface Chemistry, Polish Academy of Sciences, Niezapominajek 8, 30-239 Krakow, Poland*

Content

1. Synthetic procedures

Synthesis of 2,3-bis(2-pyridyl)quinoxaline

The synthesis was performed according to the procedure described in the literature [1]. To a solution of 2,2'-pyridyl (1.8 mmol) in absolute ethanol 1,2-phenylenediamine (1.80 mmol) was added. The resulted mixture was refluxed for 4 h. Next, the solvent was removed under reduced pressure to give the pure product **dpq** (58.5%). Anal. Calc. for $C_{18}H_{12}N_4$: C (76.04%), H (4.26%), N (19.70%), Found: C (75.59%), H (4.114%), N (19.66%).

Synthesis of 2,3-bis(2-pyridyl)benzo[g]quinoxaline

The synthesis was performed according to the procedure described in the literature [1]. To a solution of 2,2'-pyridyl (1.4 mmol) in absolute ethanol 2,3- diaminonaphthalene (1.4

mmol) was added. The resulted mixture was refluxed for 4 h. Next, the solvent was removed under reduced pressure to give the pure product **dpb** (45.3%). Anal. Calc. for $C_{22}H_{14}N_4$: C (79.01%), H (4.23%), N (16.76%), Found: C (76.59%), H (4.181%), N (16.02%).

Synthesis of $[Ru(dip)_2Cl_2]$ complex

The synthesis was performed according to the well-known literature procedure [2]. Ruthenium(III) chloride trihydrate (0.2 mmol) and 4,7-diphenyl-1,10-phenanthroline (dip) (0.4 mmol) with few drops of N-ethylmorpholine were dissolved in N,N-dimethylformamide (10 mL). The mixture was refluxed for 24 h. Then the solvent was removed under reduced pressure to c.a. 2 mL and 10 ml of acetone was added. After 24 h at -20ºC, the dark solid obtained was filtrated and washed with cold acetone, twice with diethyl ether and dried under vacuum. The crude violet product was finally purified by flash chromatography (neutral Al_2O_3, dichloromethane/methanol (2/98)) to give the pure product.

2. HPLC and HRMS data

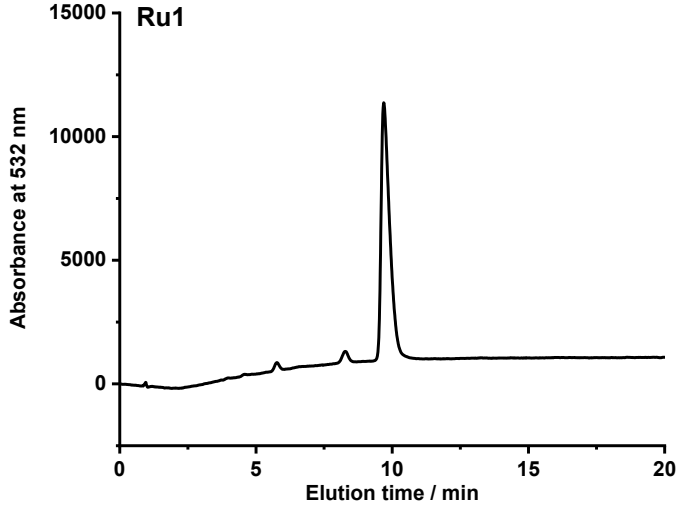

Fig. S1. The HPLC chromatogram for **Ru1**.

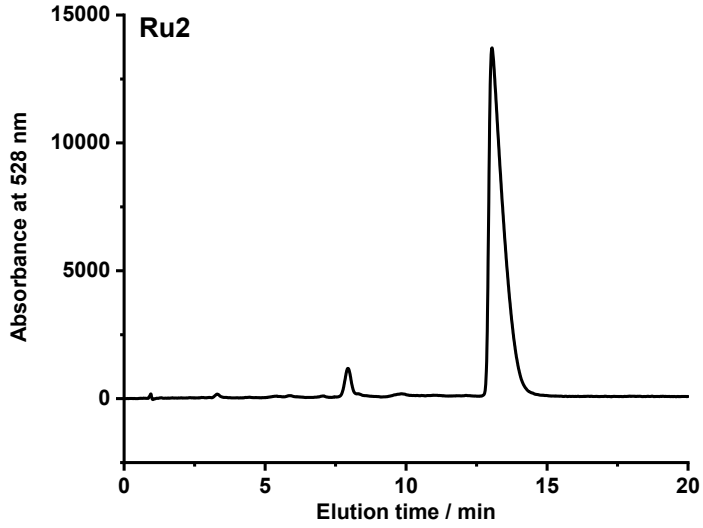

Fig. S2. The HPLC chromatogram for **Ru2**.

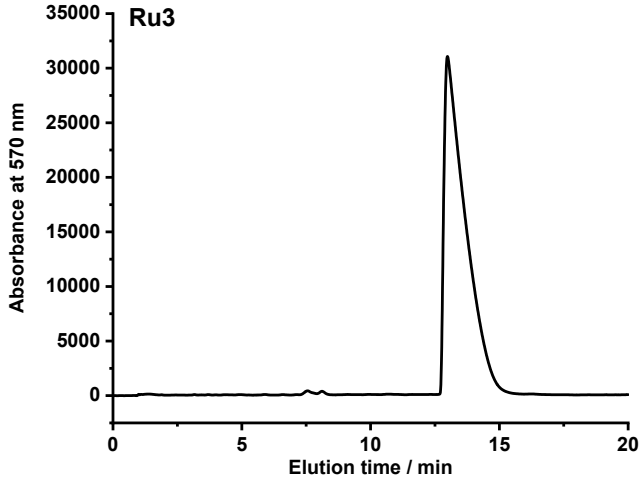

Fig. S3. The HPLC chromatogram for **Ru3**.

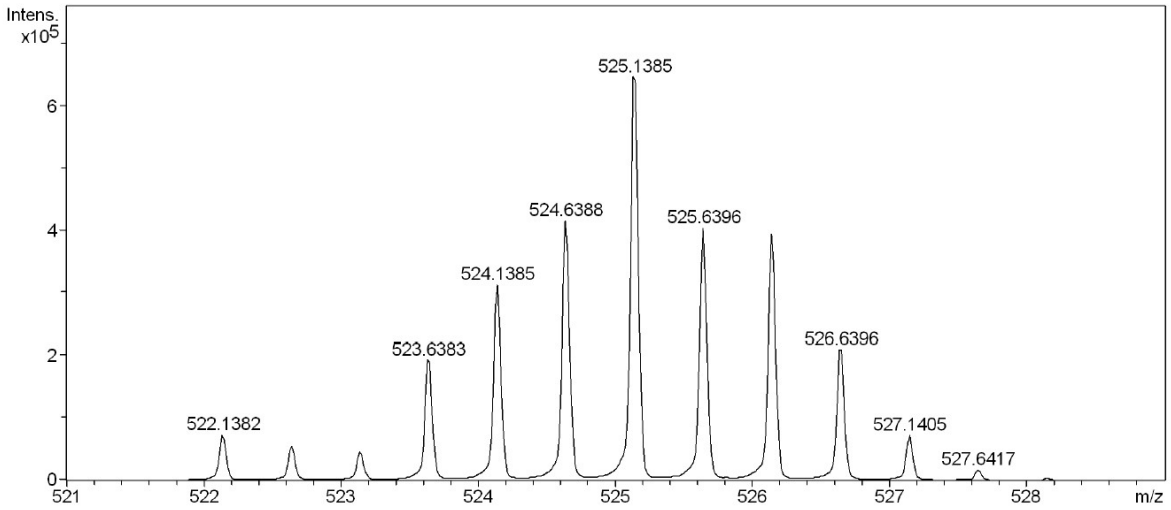

Fig. S4. HRMS spectra for **Ru1**.

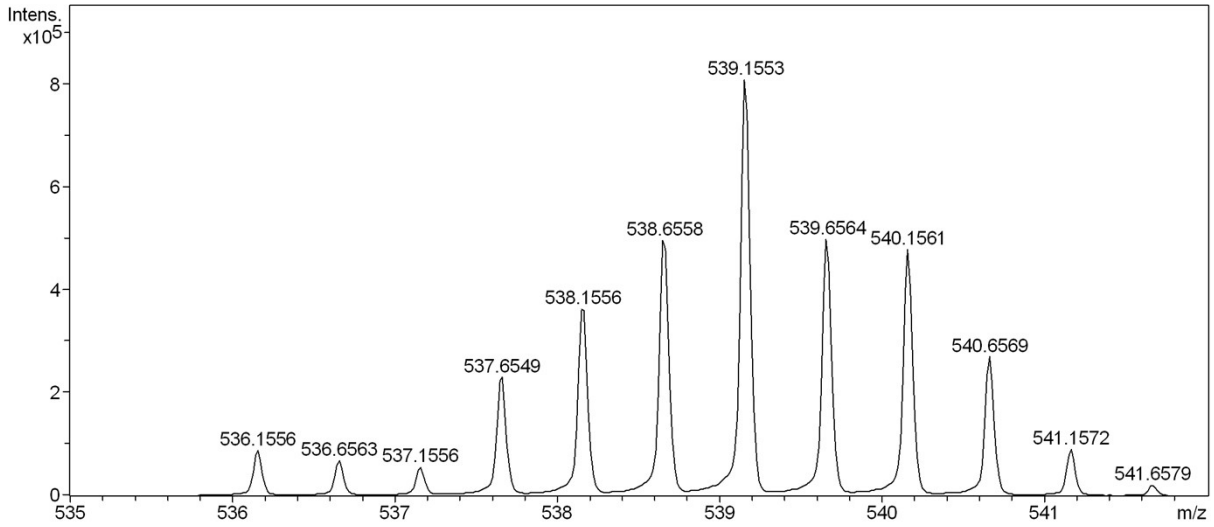

Fig. S5. HRMS spectra for **Ru2**.

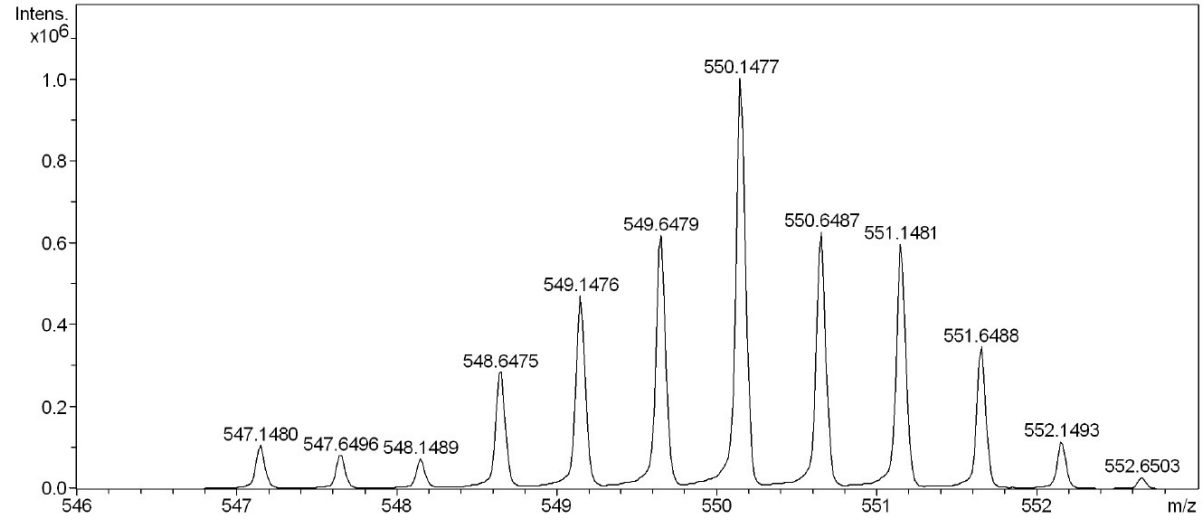

Fig. S6. HRMS spectra for **Ru3**.

3. Electronic absorption data

Table S1. Electronic absorption data for Ru(II) polypyridyl complexes in water.

	λ_{max} [nm]	ε [10^4 M^{-1} cm^{-1}]
$[Ru(dip)_2(dpq)]Cl_2$ (**Ru1**)	277	7.61 ± 0.29
	388	1.50 ± 0.91
	436	1.33 ± 0.57
	532	0.78 ± 0.03
	630[#]	0.05 ± 0.01
$[Ru(dip)_2(dpq\text{-}(CH_3)_2)]Cl_2$ (**Ru2**)	277	5.12 ± 0.59
	390	1.07 ± 0.12
	439	0.86 ± 0.10
	528	0.51 ± 0.06
	630[#]	0.04 ± 0.01
$[Ru(dip)_2(dpb)]Cl_2$ (**Ru3**)	277	9.61 ± 1.58
	395	2.25 ± 0.04
	439	1.75 ± 0.28
	570	0.91 ± 0.14
	630[#]	0.18 ± 0.02

[#]No maximum is observed, however, this wavelength is relevant for application compounds in PDT therapy.

4. DFT data for structures of the Ru1, Ru2, Ru3 complexes

Table S2. Relative total energies computed with the DFT-B3LYP/6-31G(d,p) and LANL2DZ method of two alternative geometries considered: the one in which both pyrazine and pyridyl rings of the L ligand were involved in coordination to form five-membered chelates (**Ru** structures), and the second in which two pyridyl rings were involved in seven-membered chelates (**Ru'** structures).

Structure	Relative energy [kJ/mol]
Ru1	0.0
Ru'**1**	35.3
Ru2	0.0
Ru'2	35.5
Ru3	0.0
Ru'3	36.7

A

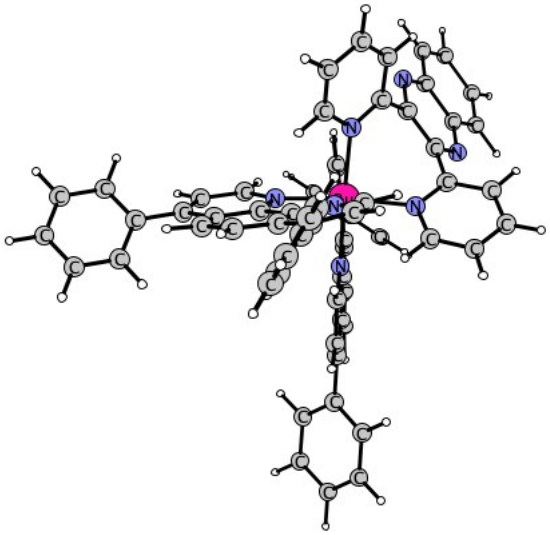

B

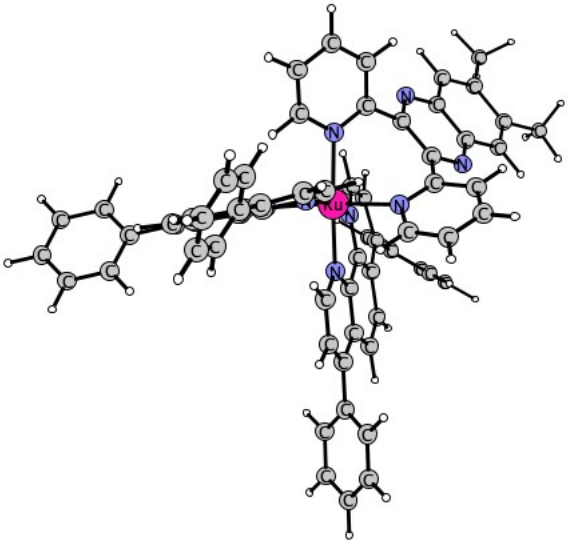

C

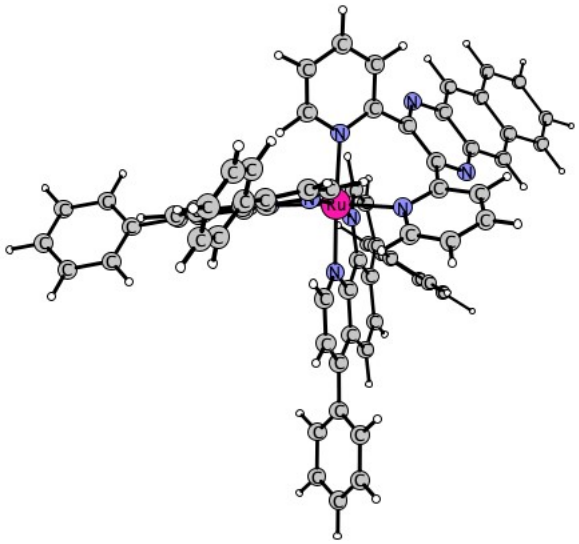

Fig. S7. Geometry structures of **Ru'1** (**A**), **Ru'2** (**B**), and **Ru'3** (**C**).

5. Photostability of the Ru complexes

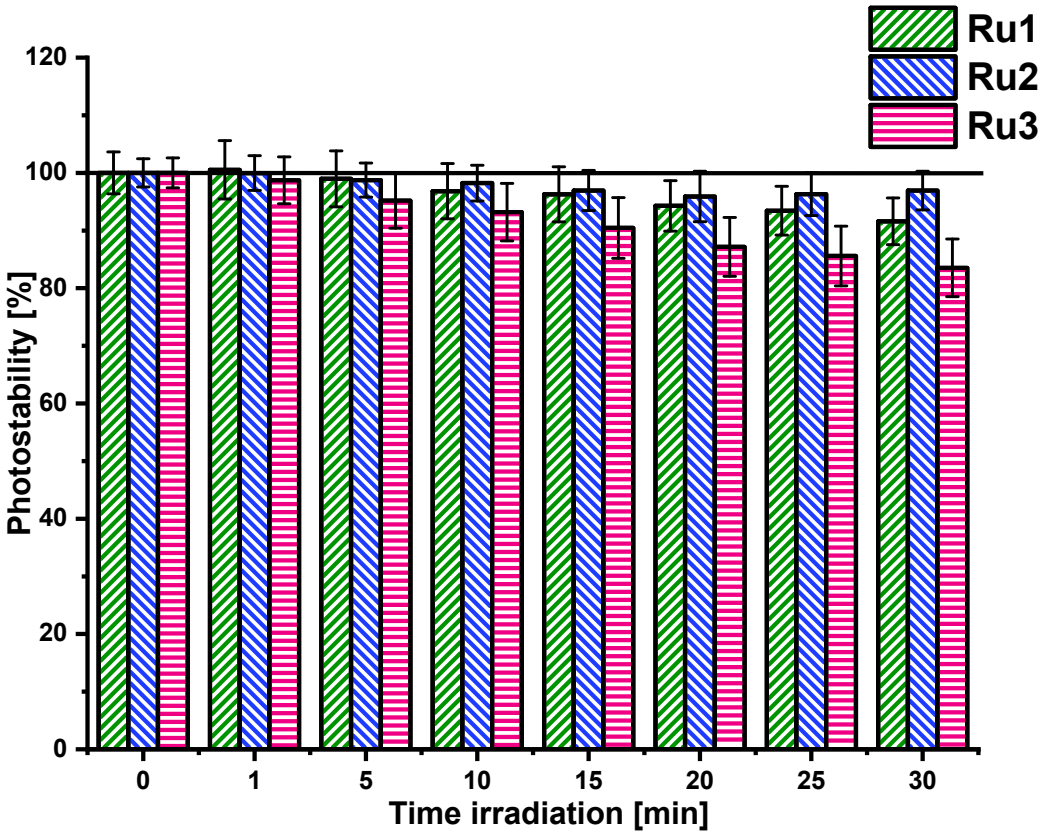

Fig. S8. Photostability of ruthenium complexes measured as changes in absorption in MLCT bands after irradiation with 465 nm light (17 mW/cm^2). [Ru] = 10-30 μM, PBS pH 7.4.

6. Uptake of the Ru complexes

cLogP values for synthesized Ru(II) complexes were estimated using a series of $[Ru(dip)_2L]^{2+}$ complexes[1]. A strong correlation (R^2 = 0.996) exists between measured $logP_{o/w}$ values for Ru(II) complexes and ones calculated for auxiliary ligands. The method was previously proved effective in case of difficulties with experimental determination of $logP_{o/w}$ for compounds.[2]

Table S3. Calculated logP for axillary ligands and Ru complexes as well as Ru accumulation in CT-26 and PANC-1 cells calculated as the ratio between [Ru] in cell (determined by ICP-MS) and [Ru] in cell medium used for cell treatment.

Compound	cLogP for (L)	cLogP for Ru complexes	$[Ru_{cell}]/[Ru_{medium}]$ CT-26	$[Ru_{cell}]/[Ru_{medium}]$ PANC-1
Ru1	2.50	0.53	38 ± 12	54 ± 18
Ru2	3.45	0.76	15 ± 4	32 ± 2
Ru3	3.68	0.81	71 ± 7	100 ± 14

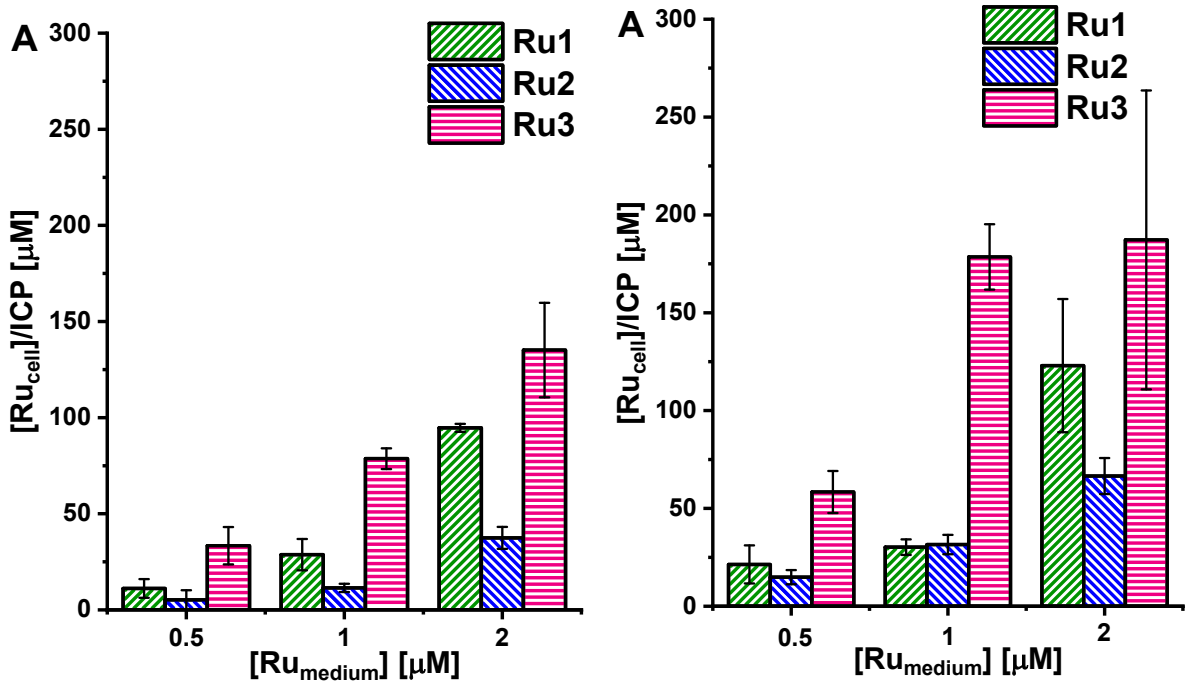

Fig. S9. Accumulation of Ru(II) complexes in CT-26 (A) and PANC-1 (B) cells was determined after 24 h incubation with the compounds.

7. Synergetic effect of the studied Ru complexes and cisplatin

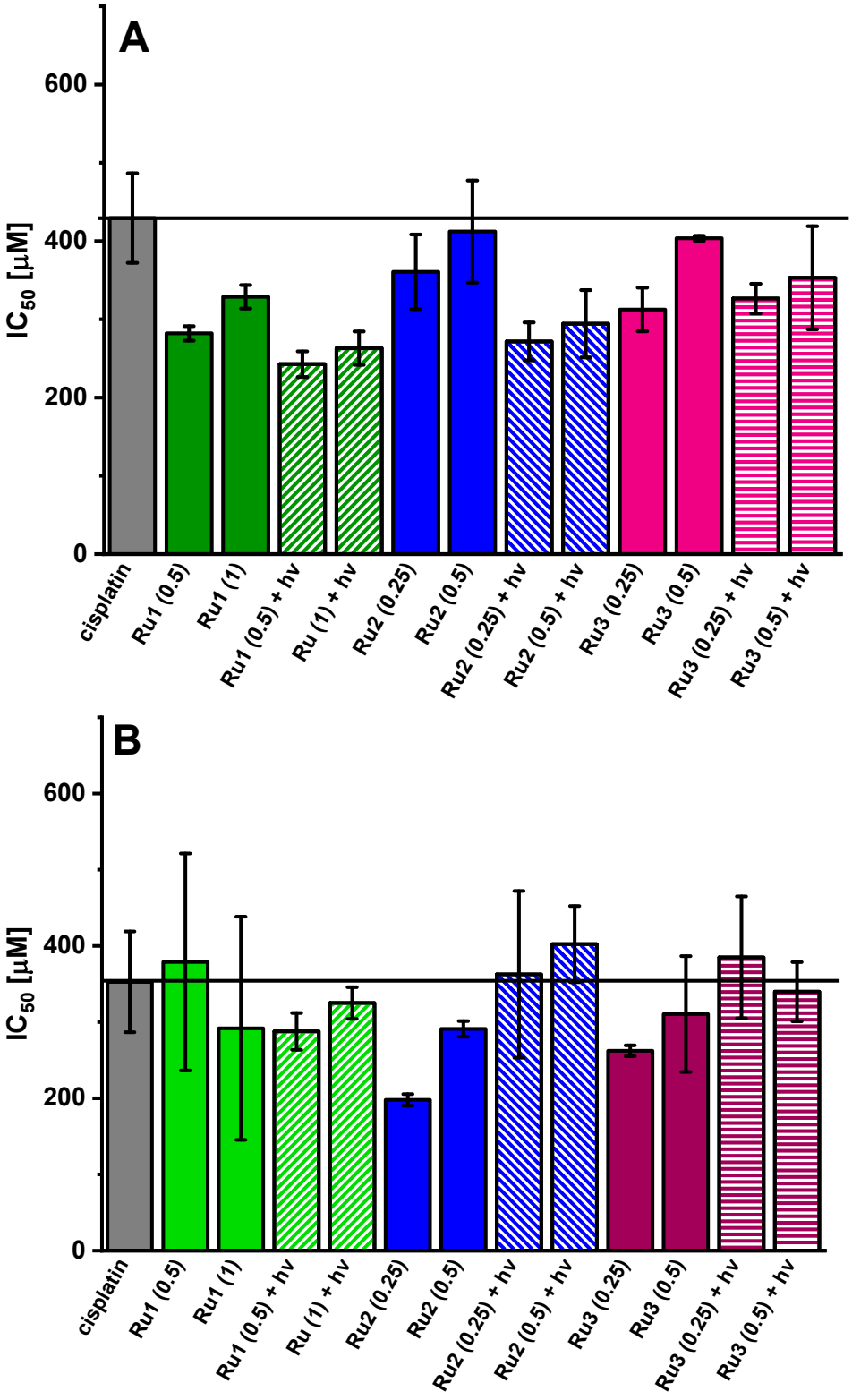

Fig. S10. Synergetic effect of tested Ru complexes combined with cisplatin evaluated on PANC-1 (A) and CT-26 (B) cells. Cells were incubated with a non-toxic concentration of Ru complexes (0.25, 0.5 or 1 μM) for 24 h at 37°C followed by washing with DPBS. Some of them were irradiated (+hυ) and all of them were incubated for the next 24 h with cisplatin.

Experimental conditions: lamp wavelength: 465 nm; lamp power 16,7 mW / cm^2, time of irradiation - 10 min.

8. Photocytotoxicity of the Ru complexes under hypoxia

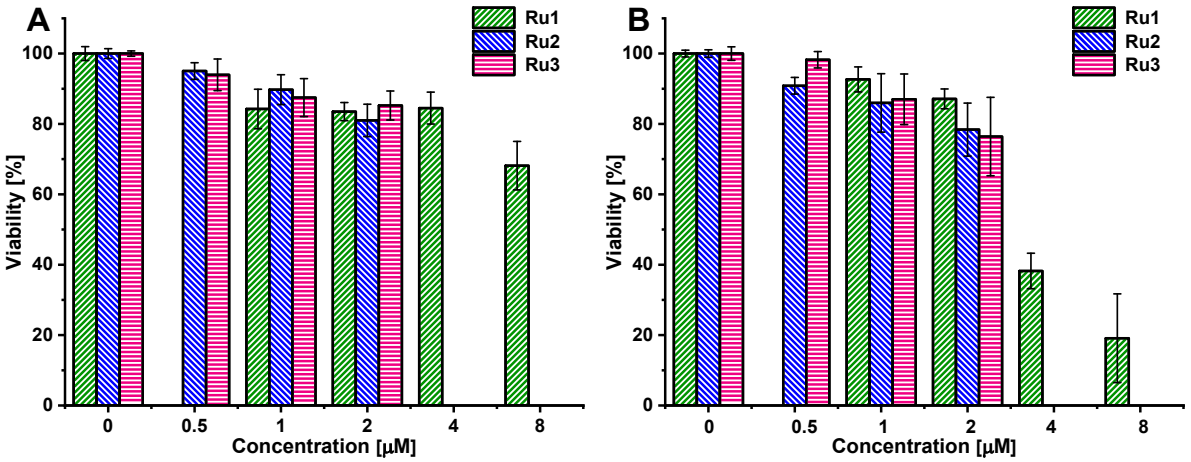

Fig. S11. Dose response plots for Ru(II) complexes in CT-26 (**A**) and PANC-1 (**B**) cell lines treated with 465 nm light (20 J/cm^2) under hypoxic conditions.

9. Reactive oxygen species generation *in vitro*

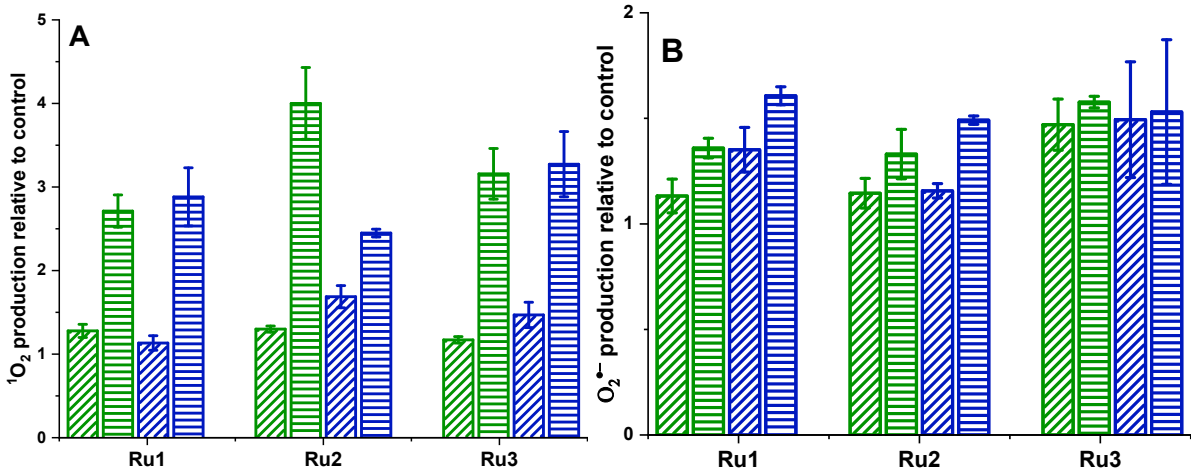

Fig. S12. Formation of reactive oxygen species upon treatment of CT-26 (green) and PANC-1 (blue) cells with 1.5 μM **Ru1**, **Ru2** or **Ru3** in the dark (oblique) or together with a visible light (horizontal) dose of 10 J/cm^2 (465 nm). The production of $^1O_2$ was assessed with SOSG (A) while $O_2^{\bullet-}$ with HE (B).

10.Cellular death mechanism

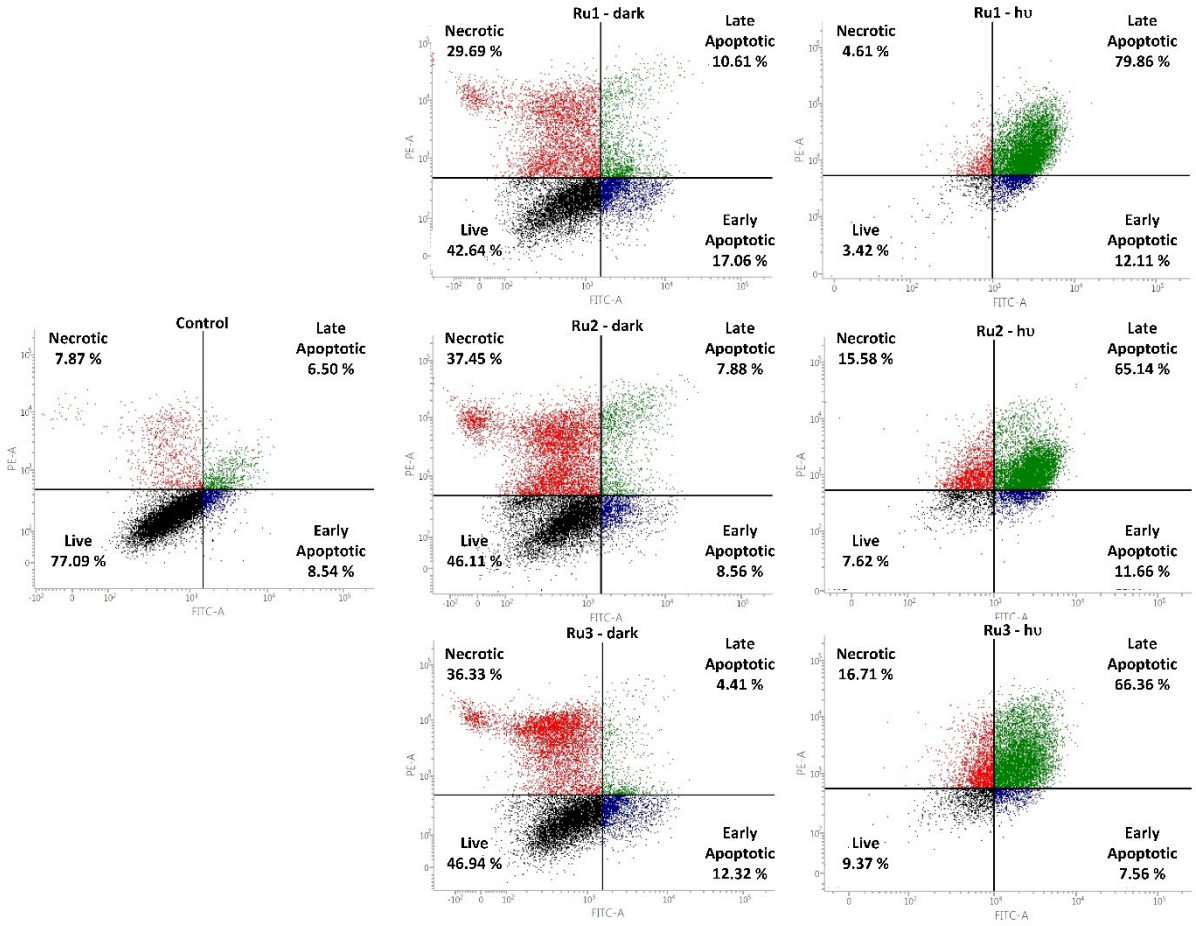

Fig. S13. The mechanism of cellular death in PANC-1 cells exposed to **Ru1-Ru3** (8 μM) in the dark or after irradiation with a visible light dose of 10 J/cm^2 (465 nm) was studied using Annexin V-FITC/PI labeling.

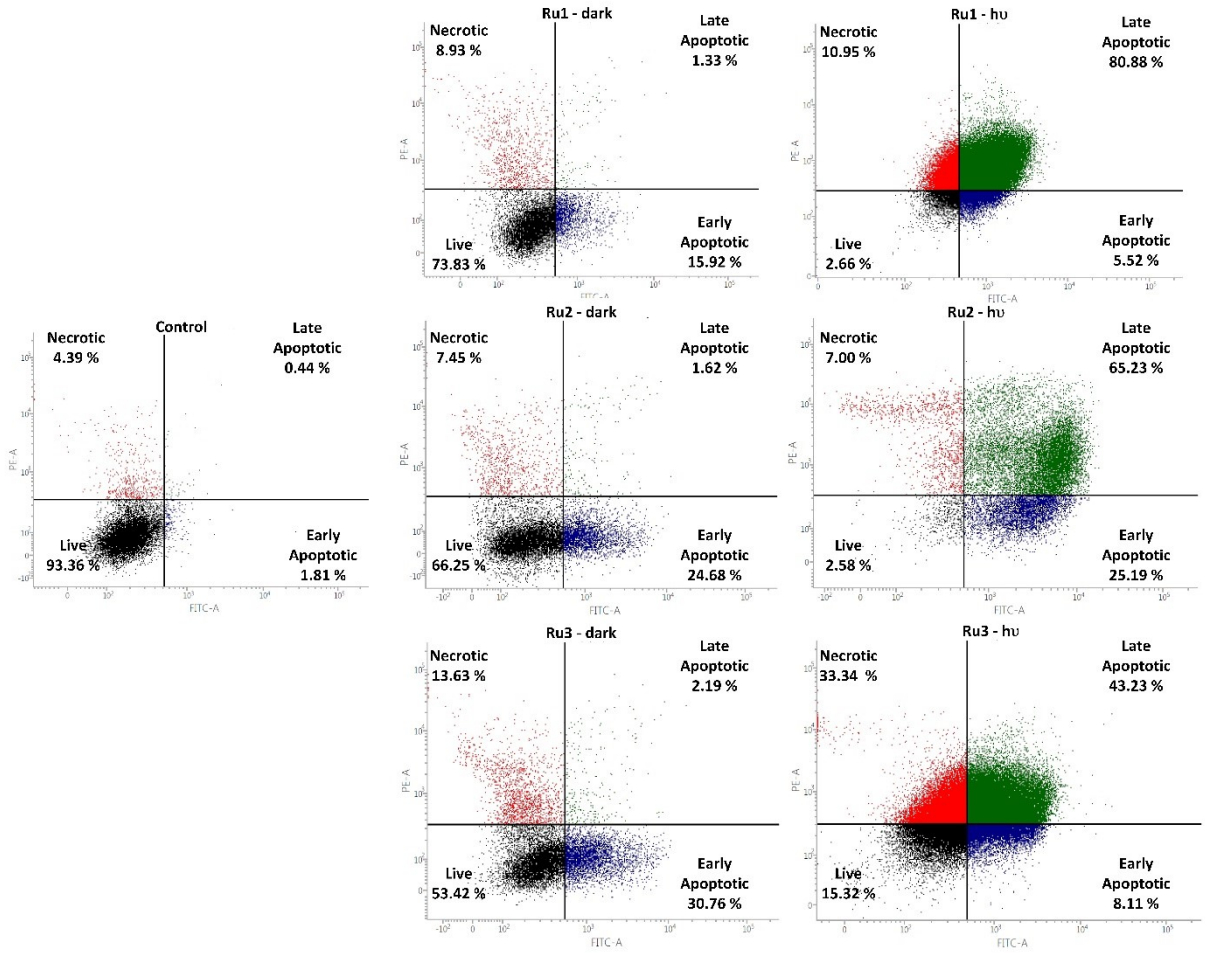

Fig. S14. The mechanism of cellular death in CT-26 cells exposed to **Ru1-Ru3** (8 μM) in the dark or after irradiation with a visible light dose of 10 J/cm^2 (465 nm) was studied using Annexin V-FITC/PI labeling.

1. O. Mazuryk, K. Magiera, B. Rys, F. Suzenet, C. Kieda and M. Brindell, *J. Biol. Inorg. Chem.*, 2014, **19**, 1305-1316.
2. I. Gurgul, O. Mazuryk, M. Łomzik, P. C. Gros, D. Rutkowska-Zbik and M. Brindell, *Metallomics*, 2020, **12**, 784-793.